Toll-like receptor 2 ligands promote microglial cell death by inducing autophagy

Daniela S. Arroyo,* Javier A. Soria,* Emilia A. Gaviglio,* Constanza Garcia-Keller,† Liliana M. Cancela,† Maria C. Rodriguez-Galan,* Ji Ming Wang,‡ and Pablo Iribarren*,[1]

*Centro de Investigaciones en Bioquímica Clínica e Inmunología (CIBICI), Consejo Nacional de Investigaciones Científicas y Técnicas (CONICET), Departamento de Bioquímica Clínica and †Instituto de Farmacología Experimental de Córdoba (IFEC), CONICET, Departamento de Farmacología, Facultad de Ciencias Químicas, Universidad Nacional de Córdoba (UNC), Córdoba, Argentina; and ‡Laboratory of Molecular Immunoregulation, Cancer and Inflammation Program, Center for Cancer Research, National Cancer Institute, Frederick, Maryland, USA

ABSTRACT **Microglial cells are phagocytes in the central nervous system (CNS) and become activated in pathological conditions, resulting in microgliosis, manifested by increased cell numbers and inflammation in the affected regions. Thus, controlling microgliosis is important to prevent pathological damage to the brain. Here, we evaluated the contribution of Toll-like receptor 2 (TLR2) to microglial survival. We observed that activation of microglial cells with peptidoglycan (PGN) from *Staphylococcus aureus* and other TLR2 ligands results in cell activation followed by the induction of autophagy and autophagy-dependent cell death. In C57BL/6J mice, intracerebral injection of PGN increased the autophagy of microglial cells and reduced the microglial/macrophage cell number in brain parenchyma. Our results demonstrate a novel role of TLRs in the regulation of microglial cell activation and survival, which are important for the control of microgliosis and associated inflammatory responses in the CNS.—Arroyo, D. S., Soria, J. A., Gaviglio, E. A., Garcia-Keller, C., Cancela, L. M., Rodriguez-Galan, M. C., Wang, J. M., Iribarren, P. Toll-like receptor 2 ligands promote microglial cell death by inducing autophagy. *FASEB J.* 27, 299–312 (2013). www.fasebj.org**

Key Words: inflammation · peptidoglycan · CNS

Autophagy is a fundamental cellular homeostatic mechanism (1), whereby cells autodigest parts of their cytoplasm for removal or turnover. During cell injury or accumulation of damaged cellular components, intracellular inclusion bodies may be transferred to the autophagic pathway, serving as a homeostatic mechanism. In autophagy, a double or multimembrane-bound structure, termed autophagosome or autophagic vacuole, is formed *de novo* to sequester cytoplasm. The vacuole membrane then fuses with the lysosome to deliver the contents into the organelle lumen, where they are degraded and the resulting macromolecules are recycled (1). Under normal conditions, cells exhibit a low basal rate of autophagy to maintain homeostasis (2). However, autophagy is increased to replenish amino acids and glucose pools for protein synthesis in response to nutrient/growth factor deprivation (nutrient recycling; refs. 3, 4). Several recent studies have implicated autophagy in the removal of pathogens located in phagosomes (5) and the cytosol (6). Moreover, a particle that engages Toll-like receptors (TLRs) on a murine macrophage while it is phagocytosed triggers the autophagosome marker light chain 3 (LC3) to be rapidly recruited to the phagosome in a manner that depends on the autophagy pathway proteins (7).

Cells may use multiple pathways to commit suicide. Apoptosis (in a broader sense called programmed cell death) means an orchestrated collapse of a cell, staging membrane blebbing, cell shrinkage, chromatin condensation, and DNA and protein degradation, accomplished by phagocytosis of corpses by neighboring cells (8). However, morphological, biochemical, and molecular observations revealed that active self-destruction of

Abbreviations: 3-MA, 3-methyladenine; 7-AAD, 7-aminoactinomycin D; AG, aminoguanidine; AnV, annexin V; APC, antigen-presenting cell; CNS, central nervous system; CPU, caudate putamen; iNOS, inducible nitric oxide synthase; KO, knockout; LAMP-1, lysosomal-associated membrane protein 1; LC3, light chain 3; LPS, lipopolysaccharide; MDC, monodansylcadaverine; MDP, muramyl dipeptide; PARP1, poly-(ADP-ribose) polymerase 1; PE, phycoerythrin; PGN, peptidoglycan; PI3K, phosphatidylinositol 3-kinase; TEM, transmission electron microscopy; TLR, toll-like receptor; TNF-α, tumor necrosis factor α; TNFR1, tumor necrosis factor receptor 1

[1] Correspondence: CIBICI-CONICET, Departamento de Bioquímica Clínica, Facultad de Ciencias Químicas, Universidad Nacional de Córdoba, Haya de la Torre y Medina Allende, Ciudad Universitaria, Córdoba X5000HUA, Argentina. E-mail: piribarr@fcq.unc.edu.ar

doi: 10.1096/fj.12-214312

This article includes supplemental data. Please visit *http://www.fasebj.org* to obtain this information.

cells is not confined to apoptosis but cells may use different pathways to commit suicide, thereby severely challenging the initial apoptosis-necrosis dichotomy (8). Recently, the autophagic-lysosomal compartment has been implicated in the initiation of programmed cell death, either upstream or independent of caspase cascade, denoted "type II programmed cell death" or "autophagic cell death" (3, 9). Caspase inhibitors are being developed as therapeutic agents for neurodegenerative diseases, such as amyotrophic lateral sclerosis (ALS; ref. 10). Recent findings indicate that caspase inhibition could have the untoward effect of exacerbating cell death and disease severity by activating the autophagic death pathway (11).

Microglial cells are resident macrophages in the central nervous system (CNS; ref. 12) and have multiple functions, such as phagocytosis, production of growth factors and cytokines, and antigen presentation (13). Acute activation of microglia after neural injury rapidly leads to reactive microgliosis, a cardinal feature of expansion of microglia in the affected CNS region (14). The increase in microglial cell number originates, in part, from recruitment of myeloid cells (14), proliferation (15), or migration from juxtaposed regions (16). The state of reactive microgliosis dissolves days to weeks later, according to an inherently tightly regulated schedule, which has been suggested to involve microglial apoptosis (17).

When pathogenic microorganisms enter the CNS, an acute edematous response ensues, as shown by localized microglial and astrocyte activation. The infection culminates in the formation of a mature abscess characterized by extensive necrosis and surrounded by a fibrous capsule (18). TLRs are germline-encoded receptors that recognize microbial pathogens (19, 20). Immediately following *Staphylococcus aureus* infection in the CNS, TLR2 is likely pivotal for microglial activation and the production of numerous chemokines and cytokines critical for the recruitment of peripheral immune cells into the site of infection and their subsequent activation (21). Recently, it was shown that stimulation of microglia with lipopolysaccharide (LPS), a TLR4 agonist, and other inflammogens activates caspase-8 and caspase-3/7 in microglia, resulting in caspase-dependent cell activation (22). These findings are in agreement with the concept that TLRs are able to induce microglial proinflammatory responses, although subtle differences may account for the effects of different TLR family members (19, 20).

In this study, we evaluated the effects of TLR2 stimulation with peptidoglycan (PGN) from *S. aureus* and other TLR2 ligands on microglial cell survival. We report that TLR2 stimulation induced, after prolonged treatment, nonapoptotic cell death through the activation of autophagy. Our findings provide new insights into the role of TLR2 in the induction of autophagy and in determining the fate of activated microglial cells.

MATERIALS AND METHODS

Reagents, cells, and animals

PGN from *S. aureus*, LPS, staurosporine, and 3-methyladenine (3-MA) were purchased from Sigma-Aldrich (St. Louis, MO, USA). Antibodies against caspase-3, poly-(ADP-ribose) polymerase 1 (PARP1), LC3B, beclin-1, and β-actin were purchased from Cell Signaling Technology (Beverly, MA, USA). Monoclonal antibodies against murine tumor necrosis factor α (TNF-α) and FasL were purchased from Becton Dickinson (San Jose, CA, USA). The caspase inhibitor zVAD-FMK was purchased from Calbiochem (Merck, Darmstadt, Germany). The murine microglial cell line BV2 was a kind gift from Dr. Dennis J. Selkoe (Harvard Medical School, Center for Neurological Diseases, Bringham and Women's Hospital, Boston, MA, USA). The murine microglial cell line N9 was a kind gift from Dr. P. Ricciardi-Castagnoli (Universita Degli Studi di Milano-Bicocca, Milan, Italy). The cells were grown in DMEM or IMDM supplemented with 10% heat-inactivated FCS, 2 mM glutamine, 100 U/ml penicillin, 100 μg/ml streptomycin, and 50 μM 2-mercaptoethanol. Primary murine microglial cells were isolated from 6- to 8-wk-old male C57BL/6J, TLR2-knockout (KO), or tumor necrosis factor receptor 1 (TNFR1)-KO mice. Animal care was provided in accordance with the procedures outlined in the U.S. National Institutes of Health (NIH) Guide for the Care and Use of Laboratory Animals (Publication 86-23, 1985). The experimental protocols were approved by the Institutional Animal Care and Use Committee of Centro de Investigaciones en Bioquímica Clínica e Inmunología (CIBICI), Consejo Nacional de Investigaciones Científicas y Técnicas (CONICET). Our animal facility obtained NIH animal welfare assurance (assurance no. A5802-01, Office of Laboratory Animal Welfare, NIH, Bethesda, MD, USA).

Isolation and treatment of primary microglial cells from adult mice

After perfusion with HBSS, brains from 6- to 8-wk-old male C57BL/6J, TLR2-KO, or TNFR1-KO mice (15 mice/group) were collected in HBSS, dispersed with scissors, resuspended in HBSS containing 0.3% collagenase D (Roche, Indianapolis, IN, USA) and 10 mM HEPES buffer (Invitrogen, Carlsbad, CA, USA), and incubated 30 min at 37°C. Brain homogenates were then filtered in 70-μm-pore cell strainers (Becton Dickinson), centrifuged (7 min, 1500 rpm), washed, and resuspended in 70% isotonic Percoll (GE Healthcare, Fairfield, CT, USA). Cell suspension (3.5 ml) was transferred to 15-ml polypropylene conical tubes with 5 ml of 25% isotonic Percoll, which were sequentially layered on top with 3 ml of PBS. After centrifugation (30 min, 800 *g*, 4°C), the 70%:25% Percoll interphase layers were collected, and the cells were washed. Finally, the adherent cells, which contained >90% of $CD11b^+$ cells, were cultured in DMEM supplemented with 10% heat-inactivated FCS, 2 mM glutamine, 100 U/ml penicillin, 100 μg/ml streptomycin, 100 μg/ml sodium pyruvate, and 10 mM HEPES buffer (Invitrogen). Microglial cells were washed with PBS and resuspended in medium containing 1% heat-inactivated FCS, PGN, or other stimuli and then cultured for the indicated times at 37°C. Morphological changes were observed in a contrast-phase microscope.

Evaluation of cell death by flow cytometry

To analyze the frequency of hypodiploid cells after stimulation, microglial cells were stained with propidium iodide as

previously reported (17). Briefly, the cells were harvested after stimulation with PGN and other molecules, fixed in 70% ethanol on ice for 30 min, and then incubated with propidium iodide (50 μg/ml) and RNase (1 mg/ml) at room temperature for 30 min. Stained cells were analyzed by flow cytometry on a FACSCanto II cytometer (Becton Dickinson).

For annexin V (AnV) and 7-aminoactinomycin D (7-AAD) dual staining, the cells were harvested, washed twice with PBS, and incubated with phycoerythrin (PE)-conjugated AnV and 7-AAD following manufacturer instructions (PE Annexin V Apoptosis Detection Kit I, Becton Dickinson). Stained cells were analyzed by flow cytometry on a FACSCanto II cytometer (Becton Dickinson).

Cytokine and nitric oxide assays

Supernatants from microglial cells stimulated with PGN and other ligands for 24 h were assayed for TNF-α production by ELISA according to the manufacturer's instructions (Mouse TNF ELISA Kit, BD Biosciences). Microglial cells were cultured in the presence or the absence of 75 μM aminoguanidine (AG; Sigma) for 1 h and then the cells were stimulated with PGN and other ligands. After 48 h, supernatants were collected and nitric oxide production was measured as nitrite using the Griess reagent (23).

Transmission electron microscopy (TEM)

Ultrastructural features of dead cells were studied by TEM as described previously (24). Briefly, microglial cells were harvested after 72 h of incubation with PGN, washed in PBS, fixed with 1% of glutaraldehyde in 0.1 M cacodylate buffer for 2 h, postfixed with osmium tetroxide at 1% in the same buffer, dehydrated, and embedded in Araldite (Huntsman Advanced Materials, Los Angeles, CA, USA). Thin sections were cut with a diamond knife on a Jeol JUM-7 ultramicrotome (Jeol Ltd., Akishima, Japan) and examined with a Zeiss LEO 906E electron microscope (Carl Zeiss, Oberkochen, Germany).

Western immunoblotting

After treatment with PGN at the indicated time points, BV2 cells were lysed with 150 μl ice-cold lysis buffer. The cell lysates were centrifuged at 14,000 rpm at 4°C for 5 min. Western blotting of caspase-3, PARP 1, LC3B, or beclin-1 was performed according to the manufacturer's instruction using specific polyclonal antibodies (Cell Signaling Technology). Briefly, proteins were electrophoresed on a 7 or 15% SDS-PAGE gel under reducing conditions and transferred onto Immun-Blot PVDF Membrane (Bio-Rad, Hercules, CA, USA). The membranes were blocked with 5% nonfat milk and 0.1% Tween-20 in TBS overnight at 4°C and then were incubated with primary antibodies for 3 h at room temperature. After incubation with a horseradish-peroxidase-conjugated secondary antibody (Cell Signaling Technology, Beverly, MA, USA), the protein bands were detected with a Super Signal Chemiluminescent Substrate (Pierce, Rockford, IL, USA) and Biomax-MR film (Eastman Kodak, Rochester, NY, USA).

Labeling of autophagic vacuoles with monodansylcadaverine (MDC)

Following stimulation with PGN, microglial cells were fixed with 2% paraformaldehyde for 5 min, washed with PBS, and then incubated with 0.05 mM MDC in PBS at 37°C for 20 min (25). After incubation, cells were washed 4 times with PBS and immediately MDC-labeled vesicles were observed by fluorescence microscopy using an inverted microscope (Nikon, Tokyo, Japan).

Surgical procedures

After 1 wk of acclimation to the housing facility, 6- to 8-wk-old male C57BL/6J mice were anesthetized with a combination of ketamine and xylazine. The mouse scalp was shaved and scrubbed with hydrogen peroxide. Animals were placed in a stereotactic frame (Thomas, Philadelphia, PA, USA). A midline incision was made, the skin was retracted, and one small borehole was drilled into the skull. The infusion cannula (30 gauge; 20 mm) was stereotaxically lowered into the caudate putamen (CPU) using the following coordinates: anterior, +0.8 mm; lateral, +1.5 mm; ventral, −3.2 mm, according to the atlas of Franklin and Paxinos (26). The infusion cannulae were connected *via* polyethylene tubing (PE 10; Becton Dickinson) to 10-μl microsyringes (Hamilton, Reno, NV, USA) mounted on a microinfusion pump (Harvard Apparatus, Holliston, MA, USA). Each mouse was injected with 0.25 μl/side at a flow rate of 0.63 μl/min. This volume was selected according to the size and structure of these nuclei. Immediately after the microinjection, the cannulae were retracted, the holes were covered with wax, and the skin was sutured with surgical thread. For *ex vivo* analysis of microglial cell death, the brains were rapidly removed and placed on ice in an acrylic brain matrix (Stoelting Co., Wood Dale, IL, USA). Coronal brain slices of 2.0 mm containing the CPU from one hemisphere were dissected. The brain tissues were homogenized with scissors on ice, and whole brain cells were costained with anti-CD45 (PE) and anti-CD11b [allophycocyanin (APC)] antibodies, AnV-FITC or AnV-PE, and 7-AAD. The frequency of AnV/7AAD$^+$ microglial cells was determined by flow cytometry gating on CD45 CD11b$^+$ cells.

Fluorescence confocal microscopy

Microglial cells grown on chamber slides were treated in the presence or absence of PGN. The cells were fixed in 4% paraformaldehyde for 10 min at room temperature and washed with PBS. The slides were then incubated with 5% normal goat serum (Sigma) in PBS, 0.05% Tween-20 (PBS-T-NGS) for 1 h to reduce nonspecific binding of antibodies to the cell surface and for cell permeabilization. An anti-LC3B (Cell Signaling Technology), anti- lysosomal-associated membrane protein 1 (LAMP-1), or anti-CD45 was applied to the slides, which were further incubated for 1 h at room temperature. After 3 rinses with PBS, the slides were incubated with Alexa Fluor 488 or Alexa Fluor 546 secondary antibodies (Invitrogen) for 60 min. The slides were analyzed under a laser scanning confocal fluorescence microscope (Olympus FV300; Olympus, Tokyo, Japan). For tissue fluorescence confocal microscopy, at different time points after surgery mice were anesthetized, perfused with 4% paraformaldehyde, and killed, and the whole brains were obtained. After treatment with sucrose, 10-μm sections were stained with anti-CD45 (Biolegend, San Diego, CA, USA), anti-LC3B (Cell Signaling Technology), or anti-LAMP-1 (Abcam, Cambridge, UK) antibodies. Alexa Fluor 488 or Alexa Fluor 546 secondary antibodies (Invitrogen) were used. The slides were analyzed under a laser scanning confocal fluorescence microscope (Olympus FV300). Quantification of microglial cell numbers in brain slides was performed using ImageJ software (NIH).

Statistical analysis

All experiments were performed ≥3 times, and the results presented are from representative experiments. The significance of the difference between test and control groups was analyzed using a 2-tailed Student's *t* test or Bonferroni's test. In all the experiments, $P < 0.05$ was considered to be statistically significant.

RESULTS

PGN induces microglial cell death

We have previously demonstrated that PGN, a cell wall component of gram-positive bacteria, activates microglial cells through TLR2 (27). Since it has been reported that TLRs may induce cell activation, caspase activation, and later apoptosis of microglial cells (22, 28), we studied the effects of PGN on mouse microglial cell survival. After 72 h of PGN treatment, we observed a decreased number of viable BV2 microglial cells (**Fig. 1*A***), which correlates with an increased frequency of hypodiploid cells (Fig. 1*B*). Then, we characterized PGN-induced microglial cell death by a kinetic evaluation of AnV *vs.* 7-AAD staining using flow cytometry. PGN increased the frequency of $AnV^+/7\text{-}AAD^+$ cells (late apoptotic/necrotic cells) after 48 h of treatment (Fig. 1*C*). However, we did not detect the presence of $AnV^+/7\text{-}AAD^-$ cells (early apoptotic cells) at any time point (Fig. 1*C*). As control, treatment of microglial cells with staurosporine, a classical apoptosis inductor, increased the frequency of early apoptotic cells (Supplemental Fig. S1*A*). We also stimulated N9 mouse microglial cell line (Supplemental Fig. S1*B*) and primary microglial cells (**Fig. 2*A***) with PGN and observed increased frequency of dead cells.

Since PGN is able to enhance the early production of proinflammatory molecules by microglial cells, such as TNF-α and nitric oxide, which in turn may induce activation-induced apoptosis of microglial cells (29–

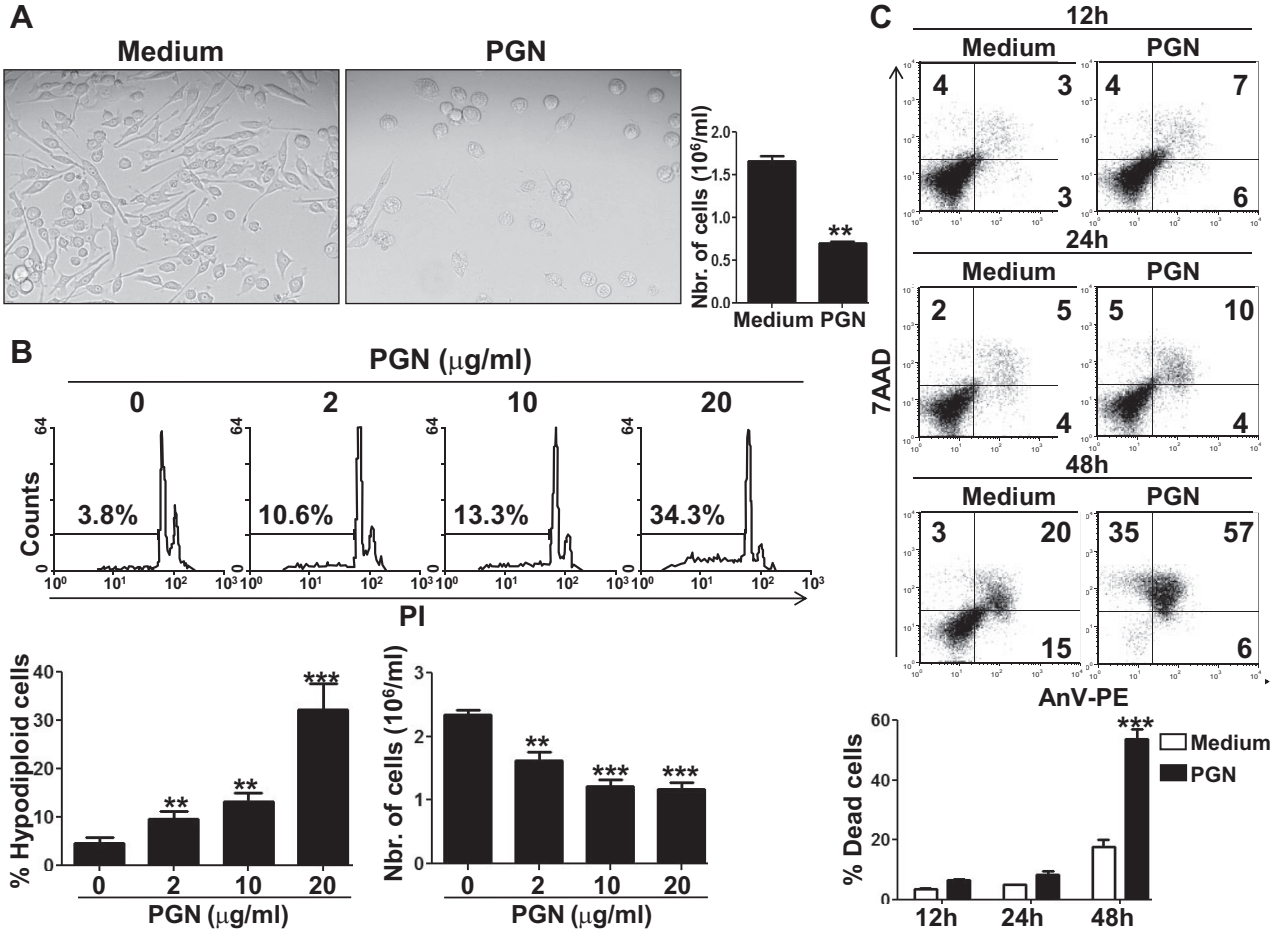

Figure 1. PGN from *S. aureus* induces microglial cell death. *A*) BV2 cells cultured in the presence or absence of PGN (20 μg/ml) for 72 h were observed with a phase-contrast microscope, and viable cells were counted. Bar graph represents means ± SD of 3 independent experiments. *B*) BV2 cells cultured for 48 h in the presence of 2, 10, and 20 μg/ml PGN were fixed with ethanol and stained with propidium iodide (PI), and the percentages of hypodiploid cells were determined by flow cytometry. Histograms of PI red fluorescence are shown; numbers indicate the frequency of hypodiploid cells. Bar graphs represent means ± SD of 3 separate experiments. *C*) BV2 cells incubated with medium or PGN (20 μg/ml) for 12, 24, or 48 h at 37°C were costained with AnV-PE and 7-AAD and analyzed by flow cytometry. Numbers in dot plots represent the percentage of cells in each quadrant. Data represent 3 independent experiments with similar results. $^{**}P < 0.01$, $^{***}P < 0.001$ *vs.* unstimulated cells.

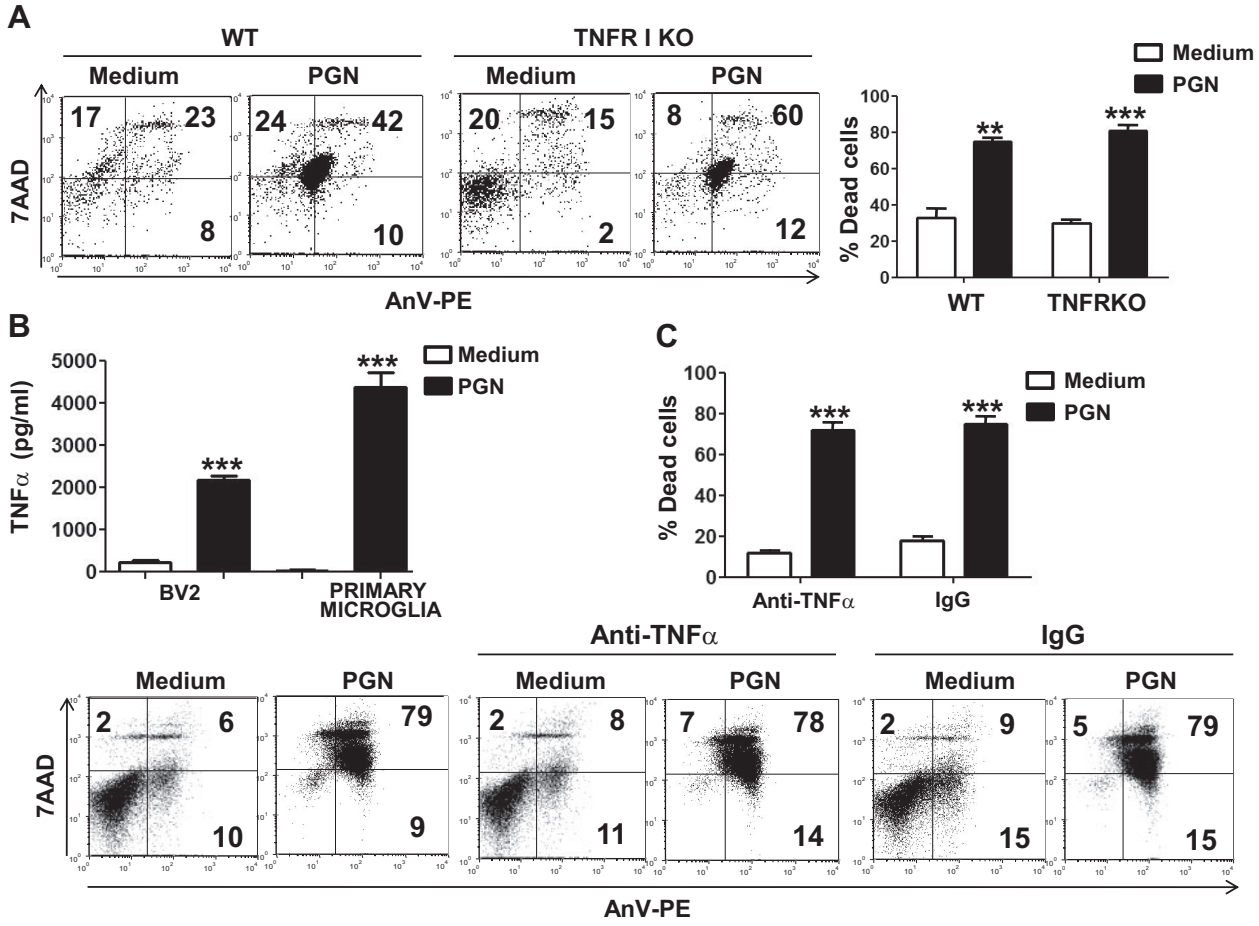

Figure 2. TNF-α is not involved in PGN-induced microglial cell death. *A*) Primary microglia from wild-type (WT) or TNFR1-KO mice cultured in the presence or the absence of PGN (20 μg/ml) for 48 h were costained with AnV-PE and 7-AAD and analyzed by flow cytometry. Numbers in dot plots represent the percentage of cells in each quadrant. Bar graphs represent mean ± SD of 3 separated experiments. *B*) Supernatants from BV2 or primary microglial cells cultured in the presence or absence of PGN (20 μg/ml) for 24 h were measured for TNF-α by an ELISA sandwich assay. ELISA data represent 3 independent experiments. *C*) BV2 cells incubated with a TNF-α-specific monoclonal antibody (10 μg/ml) or control IgG (10 μg/ml) for 1 h at 37°C were cultured in the presence or absence of PGN (20 μg/ml) for 48 h. Cells were costained with AnV-PE and 7-AAD and analyzed by flow cytometry. Numbers in dot plots represent the percentage of cells in each quadrant. Bar graphs represent means ± SD of 3 separated experiments. $^{**}P < 0.01$, $^{***}P < 0.001$ *vs.* unstimulated cells.

31), we evaluated their contribution to PGN-induced cell death. After 24 h culture in the presence of PGN, both BV2 and primary microglial cells secreted increased levels of TNF-α (Fig. 2*B*). However, a neutralizing monoclonal antibody against TNF-α did not reduce PGN-induced microglial cell death (Fig. 2*C*). These results were confirmed by using primary microglial cells isolated from both wild-type and TNFR1-deficient mice (Fig. 2*A*), suggesting that TNF-α is not involved in the PGN-induced microglia death. Similar results were obtained when microglial cells were stimulated with PGN in the presence of a neutralizing monoclonal antibody specific for Fas ligand (Supplemental Fig. S1*A*). Overall, these data suggest that microglial death induced by PGN is not mediated by TNF-α or by Fas ligand.

In another set of experiments, we observed that PGN induced increased expression of inducible nitric oxide synthase (iNOS) mRNA and protein in microglial cells (Supplemental Fig. S2*A*, *B*, respectively). The increase in iNOS expression correlated with a significant boost in nitric oxide production by microglial cells treated with PGN and also by the synthetic TLR2 ligand Pam3CSK4, effects that were blocked by the iNOS specific inhibitor AG (Supplemental Fig. S2*C*). These results led us to hypothesize that nitric oxide induced by PGN may be responsible of the death of microglia cells. However, data shown in Supplemental Fig. S2*D* may indicate that nitric oxide induced by PGN or Pam3CSK4 is not responsible of microglial cell death, as similar percentages of $AnV^+/7\text{-}AAD^+$ cells could be detected in the presence or the absence of AG**.** Moreover, polymixin B, which binds and inactivates LPS, did not inhibit PGN-induced death and nitric oxide production by microglial cells, although it efficiently blocked LPS-induced cell death and nitric oxide production in these cells (Supplemental Fig. S2*E*), suggesting that the activity of PGN is independent of possible minimal contamination with endotoxin.

Caspase-3 is a key mediator of apoptosis being re-

sponsible for the proteolytic cleavage of many key proteins such as the nuclear enzyme PARP (32). We studied the levels of caspase-3 in BV2 microglial cells after treatment with PGN. Microglial cells expressed full-length caspase-3 (35 kDa), and after 24 h treatment with LPS, the levels of cleaved caspase-3 (17–19 kDa) were increased (**Fig. 3*A***). The pan-caspase inhibitor zVAD was able to block that cleavage. In contrast to LPS, PGN only induced minimal levels of cleaved caspase-3 and the PGN-induced cell death was not blocked by zVAD (Fig. 3). All together, these results indicate that even though PGN is able to induce high levels of TNF-α and nitric oxide by microglia, these molecules may not participate in the cell death process. Moreover, our data also point out that PGN induces microglia cell death through a nonapoptotic mechanism.

Autophagy is required for PGN-induced microglial cell death

Nonapoptotic forms of cell elimination include necrosis and autophagic cell death (8). We next evaluated the morphological and ultrastructural features of the dying microglia. The dead BV2 microglial cells caused by PGN treatment appeared to be round and detached (Fig. 1*A*), and they had a plasma membrane permeable to vital dyes (Fig. 1*C*); these features differed from apoptosis, in which nuclei are condensed and membrane integrity is preserved. TEM of dead cells induced by PGN revealed disruption of outer cell membrane and numerous large cytoplasmic inclusions that were membrane-bound vacuoles characteristic of autophagy (Supplemental Fig. S3*A*, arrows). Higher magnification showed autophagic vacuoles containing a double membrane (Supplemental Fig. S3*A*, arrowhead). Moreover, we used MDC to stain autophagic vesicles in microglial cells. Treatment with PGN increased the frequency of microglial cells containing MDC-labeled vesicles (Supplemental Fig. S3*B*, arrows). The autophagy marker LC3 was originally identified as a subunit of microtubule-associated proteins 1A and 1B (termed MAP1LC3; ref. 33). Soluble LC3 (Atg8) is called LC3B I, and the detection of the lipidated, autophagosome-specific form, LC3B II, is widely used to monitor autophagy (34). Induction of autophagy in BV2 and primary mouse microglial cells was monitored with morphometric analysis after the formation of LC3B-labeled autophagosomes (≥1 μm; ref. 35). Culture of both BV2 (**Fig. 4**) and primary (see Fig. 7) microglial cells with PGN resulted in a significant increase in the number of $LC3B^+$ puncta per cell (Figs. 4*C*, *G* and 7*A*, *B*, respectively). Interestingly, the PGN-induced formation of LC3 puncta was blocked by the addition of LY294002, a specific pan-phosphatidylinositol 3-kinase (PI3K) inhibitor (Figs. 4*D*, *G* and 7*A*, *B*, respectively). Since PGN activates TLR2 in microglial cells, we evaluated the capacity of synthetic TLR2 ligand Pam3CSK4 (TLR2/6 agonist) to mimic the effects of PGN. Pam3CSK4 induced a significant increase in the number of $LC3B^+$ puncta per cell, and here again, this effect was blocked by the addition of LY294002 (Fig. 4*E–G*).

The PGN-induced autophagy was confirmed by an

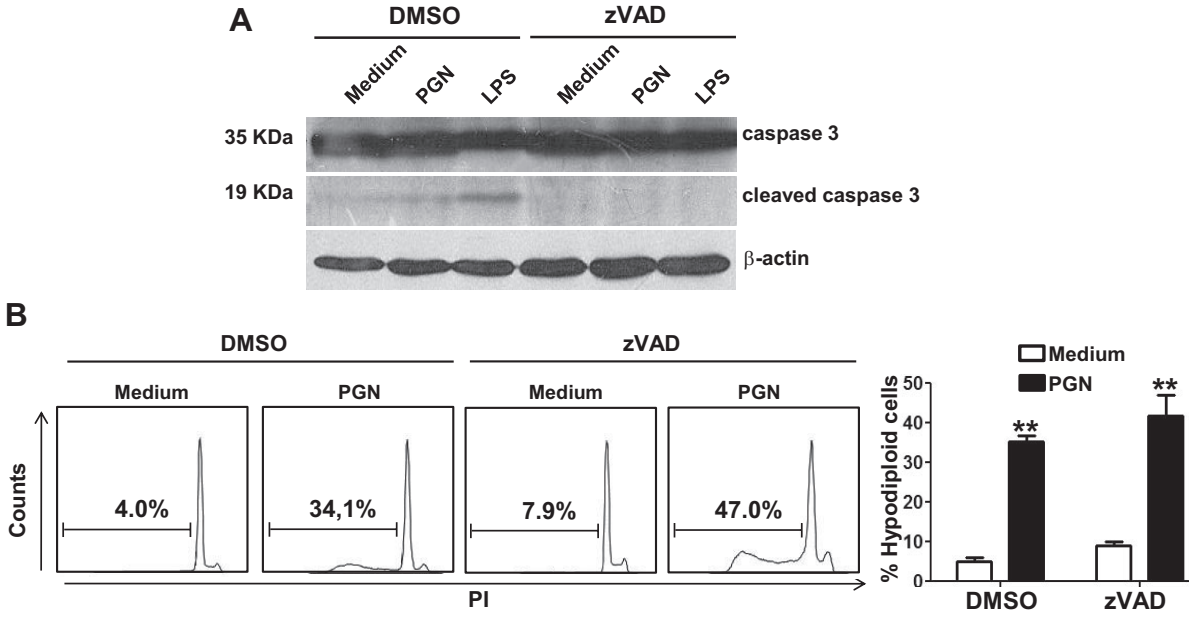

Figure 3. Caspase activation is not required for PGN-induced microglial cell death. *A*) BV2 cells incubated in the presence of zVAD (20 μM; a pan-caspase inhibitor) or DMSO for 1 h at 37°C were cultured in the presence or absence of PGN (20 μg/ml) or LPS (1 μg/ml) for 24 h at 37°C. Cells were lysed, and caspase-3 was examined by Western immunoblotting. Results represent ≥3 independent experiments. *B*) BV2 cells cultured in the presence of zVAD or DMSO for 1 h at 37°C were stimulated with PGN for 48 h. Cells were fixed with ethanol and stained with PI, and the percentages of hypodiploid cells were evaluated by flow cytometry. Histograms of PI (red fluorescence) are shown; numbers indicate the frequency of hypodiploid cells. Bar graphs represent means ± SD of 3 separate experiments. $^{**}P < 0.01$ *vs.* unstimulated cells.

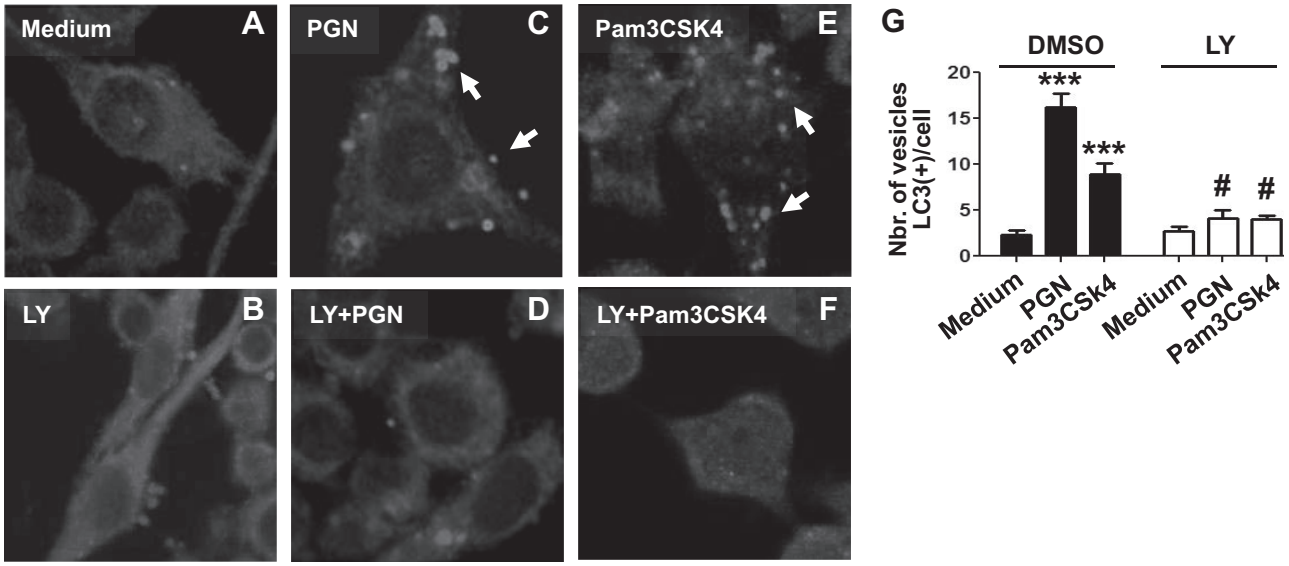

Figure 4. Authophagy is shown by microglial cells stimulated with PGN. BV2 cells were incubated in the presence of DMSO (*A*) or LY294002 (LY; 50 μM; a PI3K inhibitor; *B*) for 1 h at 37°C. These cells, cultured in the presence or absence of PGN (*C, D*) or Pam3CSK4 (*E, F*; 5 μg/ml) for 24 h were stained with an LC3B-specific antibody and evaluated using a confocal fluorescence microscope. Arrows indicate the presence of $LC3B^+$ punctated cells. Bar graph (*G*) represents means ± SD of the number of $LC3^+$ vesicles per cell of 3 separate experiments. $^{***}P < 0.001$, $^{\#}P > 0.05$ (nonsignificant) *vs.* unstimulated cells.

assay that measures conversion of LC3B I (nonlipidated form with lower electrophoretic mobility) to LC3B II (LC3 form C-terminally lipidated by phosphatidylethanolamine, displaying higher electrophoretic mobility) with immunoblots (34). As expected, induction of microglial autophagy by PGN increased the intensity of the LC3B II relative to the intensity of LC3B I band (**Fig. 5*A***). When 3-MA, a specific inhibitor of early stages of autophagy, was added to PGN-stimulated microglial cell cultures, the intensity of the LC3B I band increased (Fig. 5*A*, compare lanes 3 and 2), indicative of a reduced LC3B I to LC3B II conversion, consistent with the inhibition of autophagy induction. In addition, PGN up-regulated beclin-1 protein, a molecule involved in the induction of autophagy (Fig. 5*A*), and this effect was not affected by the addition of 3-MA, indicating that PGN is able to modify beclin-1 expression independently of the autophagy response.

PARP1, an enzyme involved in DNA base-excision repair, is cleaved and inactivated by caspase-3 (36). Necrosis is characterized by an overactivation of PARP1 and its subsequent cleavage into a major fragment of 55 kDa (37). We observed that untreated microglial cells expressed low levels of a 55-kDa fragment, which were increased after the treatment with PGN (Fig. 5*B*). Interestingly, in the presence of 3-MA, both untreated and PGN-treated microglial cells contained the full-length PARP 1 (116 kDa) and a cleaved 89-kDa fragment, suggesting caspase activation (Fig. 5*B*). Moreover, the levels of the full-length caspase-3 in microglial cells decreased in the presence of 3-MA (Fig. 5*B*). As expected, the caspase-mediated cleavage of PARP 1 and the decrease in the levels of full-length caspase-3 were inhibited by the caspase inhibitor zVAD (Fig. 5*B*). The PGN-induced microglial cell death was blocked by either 3-MA or LY294002, indicating that the induction of autophagy is required for the killing of microglial cells by PGN (Fig. 5*C*). In another set of experiments, we found that both Pam2CSK4 (TLR1/2 agonist) and Pam3CSK4 increased microglial cell death with a necrotic staining pattern (**Fig. 6**). The presence of 3-MA or LY294002 prevented the induction of microglial cell death by both Pam2CSK4 and Pam3CSK4 (Fig. 6). Muramyl dipeptide (MDP) is the minimally bioactive PGN motif common to all bacteria and has been shown to be recognized by NOD2, but not TLR2, nor TLR2/1 or TLR2/6 associations (38). Stimulation of microglial BV2 cells with MDP failed to induce cell death (Fig. 6 and Supplemental Fig. S2*D*). To confirm the involvement of TLR2 in the killing effects of PGN, we studied autophagy response and cell death of primary microglial cells obtained from TLR2-KO mice. As we expected, PGN failed to increase the number of $LC3B^+$ puncta per cell (Fig. 7*A, C*) in TLR2-KO microglial cells but induced $LC3B^+$ autophagic vesicles in wild-type microglial cells (**Fig. 7*A***, *C*). In addition, PGN failed to induce cell death of TLR2-KO microglial cells, but as previously shown, it is able to induced cell death of wild-type microglial cells (Fig. 7*D*). Overall, these results suggest that activation of TLR2 by PGN induces autophagy and autophagy-dependent microglial cell death.

Microglial/macrophage cell depletion and increased autophagy are induced by PGN *in vivo*

To evaluate whether *in vivo* TLR2 stimulation is able to induce microglial cell death and autophagy, we injected PGN into the mouse brain parenchyma (CPU). At different time points, brains and CPU were analyzed

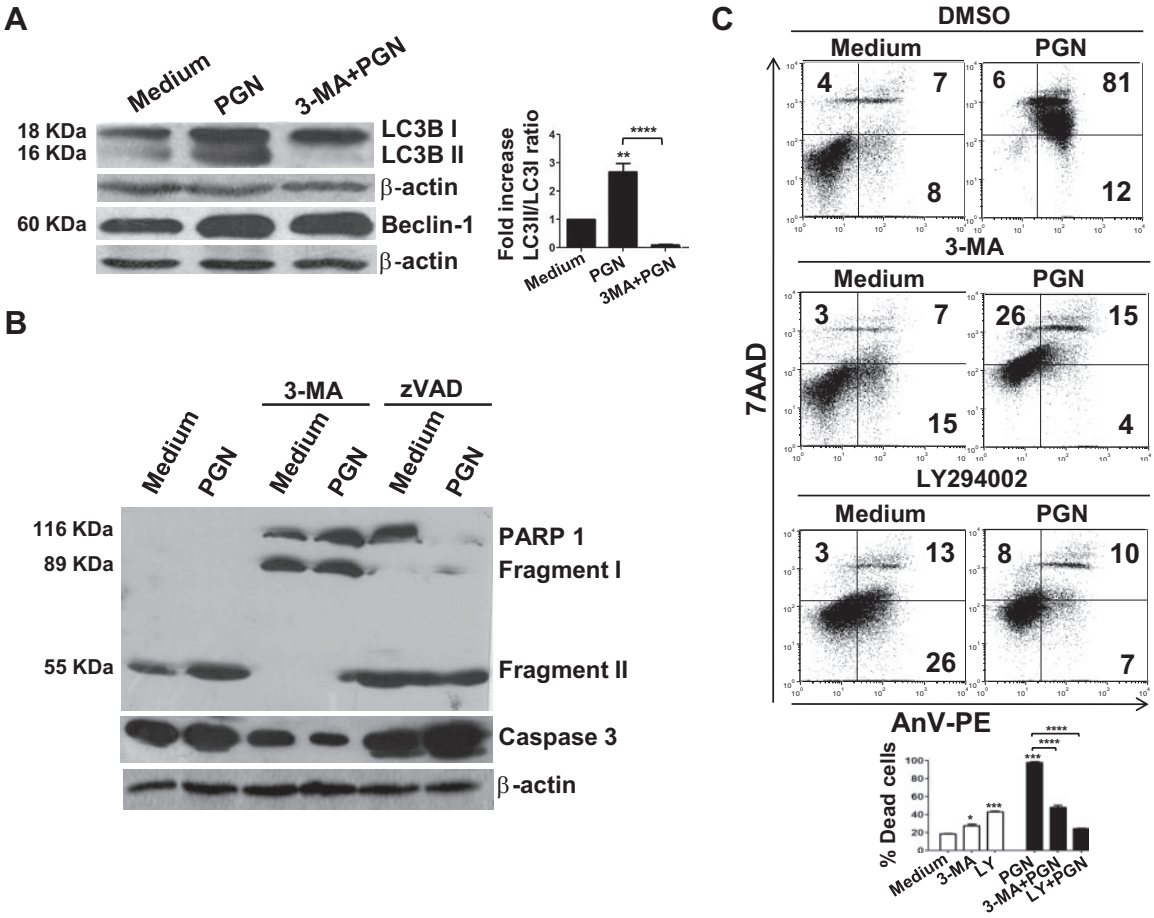

Figure 5. PGN-induced microglial cell death requires autophagy. *A*, *B*) BV2 cells incubated with 3-MA (2.5 mM; a specific inhibitor of autophagy), zVAD (20 μM), or DMSO for 1 h at 37°C were cultured in the presence or absence of PGN (20 μg/ml) for 24 h at 37°C. Cells were lysed, and LC3B, beclin-1, PARP 1, caspase-3, and β-actin were examined by Western immunoblotting. Data are representative of ≥3 independent experiments with similar results. *C*) BV2 cells incubated with 3-MA, LY294002 (LY) or DMSO for 1 h at 37°C were cultured in the presence or absence of PGN for 48 h. Cells were then costained with AnV-PE and 7-AAD and analyzed by flow cytometry. Numbers in dot plots represent the percentage of cells in each quadrant. Bar graphs represent means ± SD of 3 separate experiments. $*P < 0.05$, $**P < 0.01$, $***P < 0.001$ *vs.* unstimulated cells; $****P < 0.001$ *vs.* PGN-stimulated cells.

for the presence of microglia in serial sections through the needle track, and 1–2 mm ventral to the end of the needle mark. The injection sites were defined as the last section containing a visible needle track and the next section without the needle artifact. Staining brain sections with CD45 allowed us to distinguish microglia and macrophage cells from astrocytes, oligodendrocytes, and neurons. In CNS leukocyte preparations, CD45 is used to separate the $CD45^{hi}$ hematogenous population from $CD45^{lo}$ resident microglia by flow cytometry. Since CD45 expression could change on monocytes and CNS-born microglial cells after proinflammatory stimulation, making difficult to distinguish between these two cell types (39), we decided to use anti-CD45 or anti-CD45 plus anti-CD11b antibodies to detect microglia/macrophages in CPU. PGN injection resulted in a significant increase in the number of $LC3B^+$ cells containing punctate structures in the brain parenchyma (**Fig. 8*A, B, E***). Moreover, the LC3 expression colocalized with the late endosomal or lysosomal marker LAMP-1 (Fig. 8*A, B, E*), indicating the fusion of autophagosomes with lysosomes. Furthermore, we confirmed that $CD45^+$ microglia/macrophages showed increased LC3B puncta after PGN injection (Fig. 8*C–E*). In addition, coinjection of PGN and LY294002 was unable to cause the increase of LC3B punctate parenchymal microglia (data not shown). We additionally evaluated microglial/macrophage cell death by flow cytometry and microglia/macrophage numbers in the parenchyma of brain sections. We found that PGN injection into the CPU induced increased frequency of $CD11b^+/CD45^+$ microglial/macrophage cell death at 48 h postinjection, reaching a peak level of cell death at 72 h (**Fig. 9*A***). Moreover, as we found in the *in vitro* studies, the staining profile corresponded to a nonapoptotic type of cell death ($AnV^+/7\text{-}AAD^+$ cells; Fig. 9*A*). In addition, we observed by flow cytometry a decrease in the frequency of $CD45^{lo}$ microglial cells after PGN injection (data not shown). These results correlated with the observation that the number of $CD45^+$ microglia/macrophages close to the vicinity (next 3 sections without the needle artifact) of the site of injection

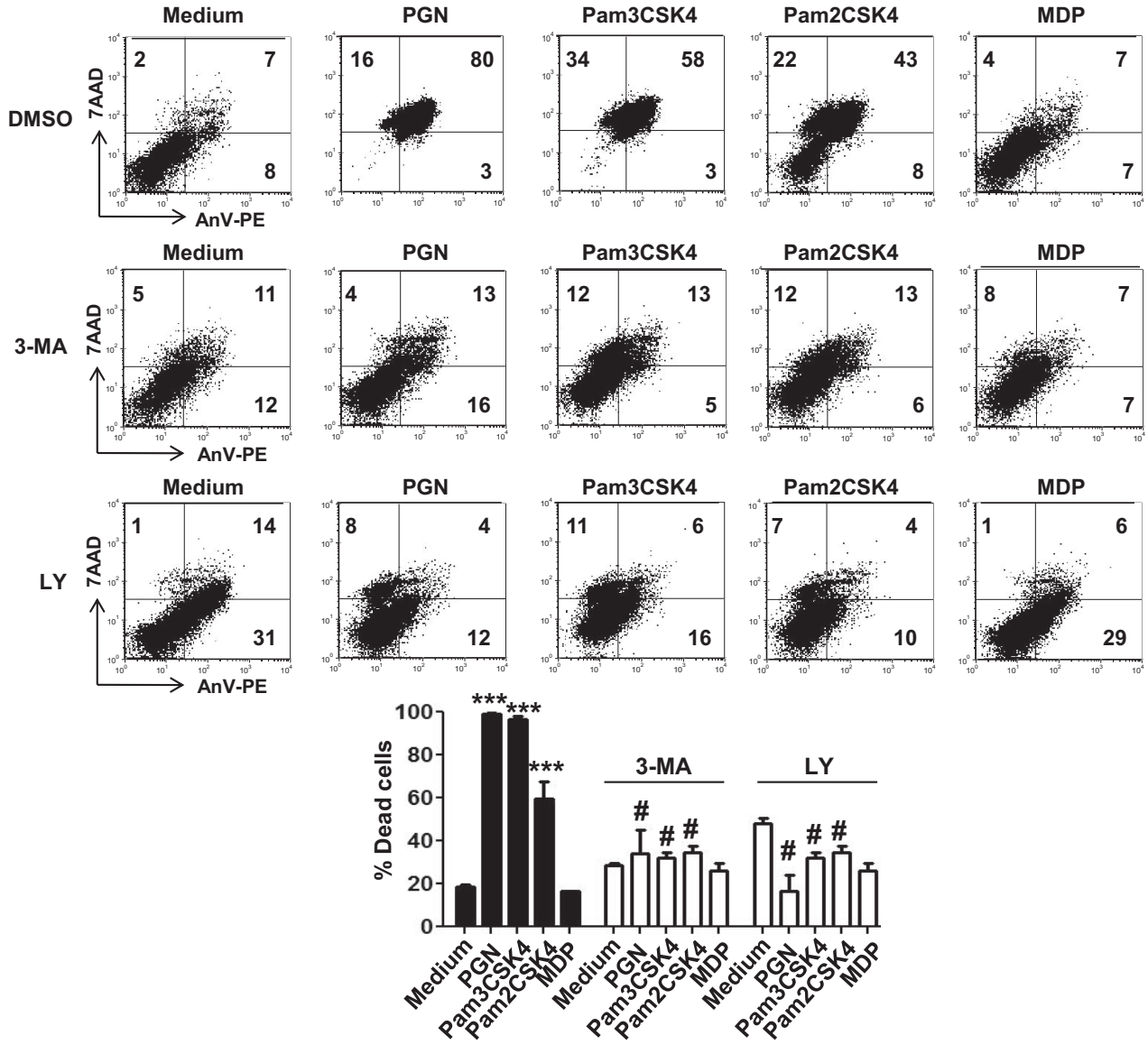

Figure 6. Synthetic TLR2 ligands induce microglial cell death. BV2 cells incubated with 3-MA, LY294002, or DMSO for 1 h at 37°C were cultured in the presence or absence of PGN (20 μg/ml), Pam2CSK4 (100 ng/ml), Pam3CSK4 (5 μg/ml), or MDP (20 μg/ml) for 48 h at 37°C. Then the cells were costained with AnV-PE and 7-AAD and analyzed by flow cytometry. Numbers in dot plots represent the percentage of cells in each quadrant. Bar graphs represent means ± SD of percentage of dead cells of 3 separated experiments. Solid bars indicate control cells incubated with DMSO. ***$P < 0.001$ *vs.* unstimulated cells; $^{\#}P < 0.001$ *vs.* cells stimulated in the absence of inhibitors.

(CPU), decreased after the injection of PGN (Fig. 9*B*). Taken together, both *in vitro* and *in vivo* experiments demonstrate that PGN is able to induce microglial cell death by mechanisms involving autophagy. Thus, PGN might act as a regulator of microglial cell survival through the induction of autophagic cell death in pathological conditions where PGN, or other TLR2 ligands, are present in the CNS.

DISCUSSION

Control of microglial cell activation and the number of activated microglial cells is crucial for the regulation of the inflammatory responses and the host defense in the CNS.

In this study, both *in vitro* and *in vivo* experiments demonstrate that activation of microglial cells with bacterial PGN and other TLR2 ligands results initially in microglial cell activation and later in the induction of microglial cell death by mechanisms involving autophagy. Thus, PGN might act as a regulator of microglial cell survival through the induction of autophagic cell death in pathological conditions where PGN, or other TLR2 ligands, are present in the CNS. To our knowledge, this is the first demonstration that activation of TLR2, an important pattern recognition receptor involved in host defense and neurodegeneration, induces autophagic cell death in microglial cells.

Microglia rapidly respond to endogenous (*e.g.*, dam-

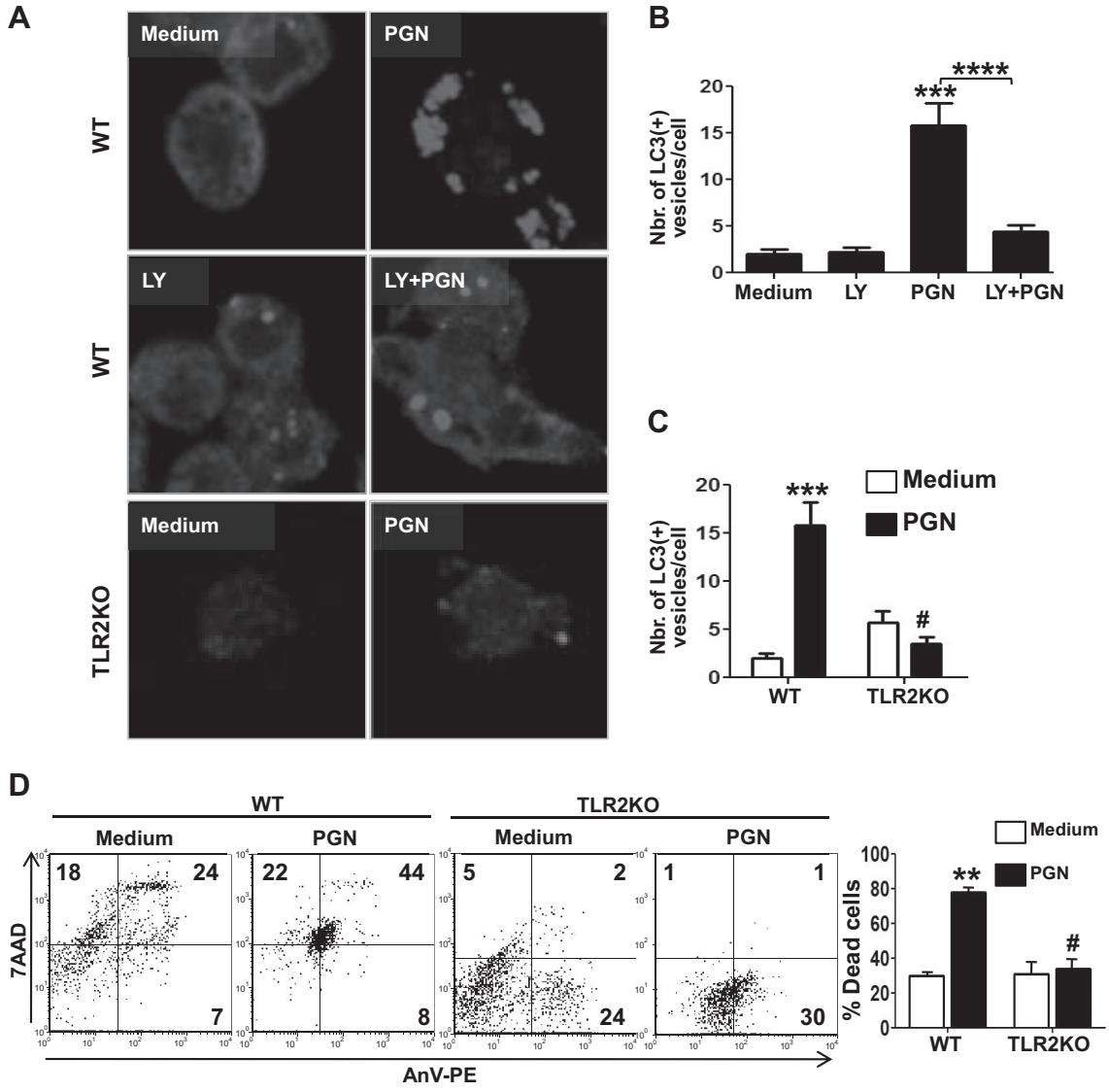

Figure 7. PGN-induced autophagy and microglial cell death require TLR2. *A*) Primary microglia from wild-type (WT) mice were incubated in the presence of LY294002 (50 μM; a PI3K inhibitor) or DMSO for 1 h at 37°C and cultured in the presence or the absence of PGN (20 μg/ml) for 24 h. Primary microglia from TLR2-KO mice were cultured in the presence or the absence of PGN (20 μg/ml) for 24 h. These cells were stained with an LC3B-specific antibody and evaluated using a confocal fluorescence microscope. *B*, *C*) Bar graphs represent means ± SD of the number of $LC3^+$ vesicles per cell of 3 separate experiments. *D*) Primary microglia from WT or TLR2-KO mice cultured in the presence or the absence of PGN (20 μg/ml) for 48 h were costained with AnV-PE and 7-AAD and analyzed by flow cytometry. Numbers in dot plots represent the percentage of cells in each quadrant. Bar graphs represent means ± SD of 3 separate experiments. $^{**}P < 0.01$, $^{***}P < 0.001$, $^{\#}P > 0.05$ (nonsignificant) *vs.* unstimulated cells; $^{****}P < 0.001$ *vs.* PGN-stimulated cells.

aged cells, cytokines, and tumors), as well as exogenous (infectious agents and endotoxin), stimuli and actively participate in immune responses, inflammation, and tissue repair in the CNS (40, 41). During these processes, microglia express markers also showed on differentiated macrophages and display effector functions including secretion of proinflammatory and neurotoxic mediators (42). Activated microglial cells also accumulate at sites of inflammation in CNS, including multiple sclerosis (43), AIDS encephalitis (44), prion disease, and Alzheimer's disease (45). Apoptosis has been suggested as an important mode of microglial population control, which is mediated through a nonclassic pathway that does not culminate in condensed fragmented DNA (46). Wirenfeldt *et al.* (47) demonstrated that apoptosis does play a role in the control of microglial population in brain regions, displaying a dense anterograde axonal and terminal degeneration in both resident and immigrating microglia. In our present study, we show that stimulation of TLR2 in microglial cells first triggers cell activation and later cell death. Since PGN-stimulated microglial cells were double-positive for AnV and 7-AAD, we conclude that PGN induced a nonapoptotic form of microglial cell death.

Cell death is an integral part of the life of an organism. However, if cell death is allowed to proceed,

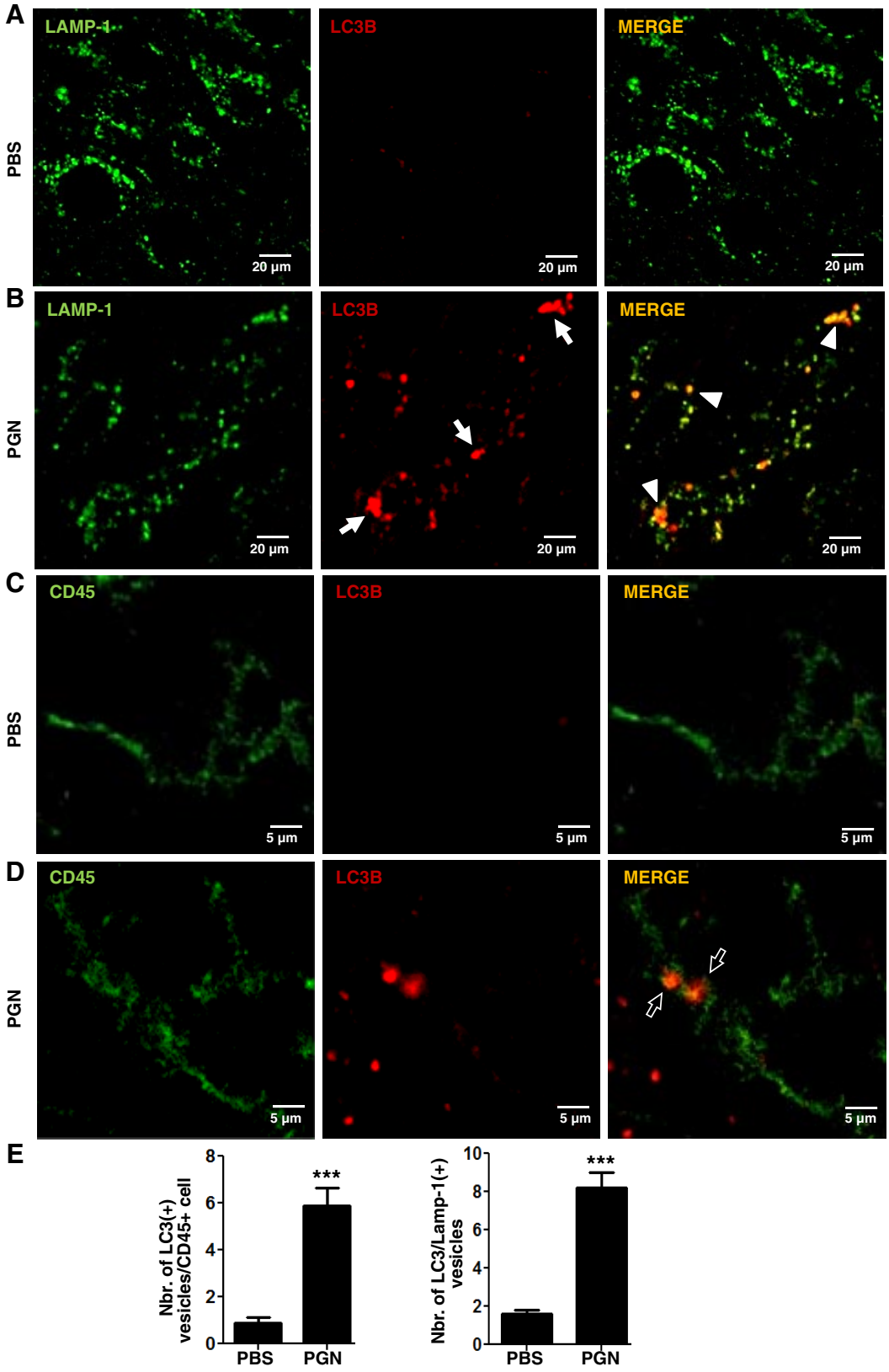

Figure 8. PGN induces microglial cell autophagy *in vivo*. PBS (*A*, *C*) or PGN (*B*, *D*) was stereotaxically injected into the mouse CPU. After 24 h, 10-μm brain sections were stained with anti-LAMP-1 (green; *A*, *B*) or anti-CD45 (green; *C*, *D*) plus anti-LC3B (red) antibodies. Alexa Fluor 488 or Alexa Fluor 546 secondary antibodies were used. Slides were analyzed under a laser scanning confocal fluorescence microscope. Arrows indicate the presence of $LC3B^+$ punctated cells. Arrowheads indicate colocalization of $LC3B^+$ vesicles with LAMP-1. Bar graphs (*E*) represent means ± SD of number of $LC3^+$ vesicles per $CD45^+$ cell of 3 separate experiments. Number of LC3/Lamp-1 double-positive cells was obtained from 10 fields/slide, analyzing the next 3 sections without the needle artifact of 3 separate experiments. $^{***}P < 0.001$ *vs.* unstimulated cells.

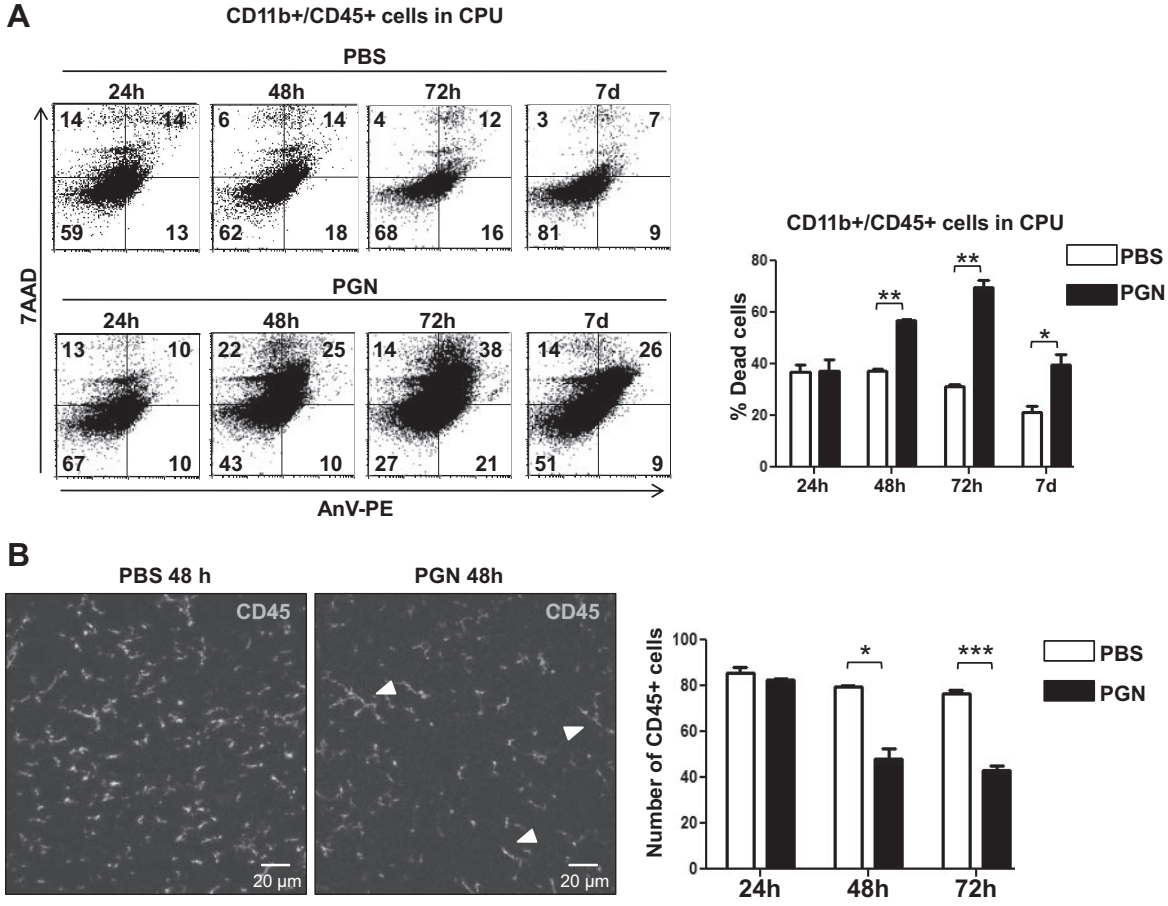

Figure 9. Microglial and macrophage cell depletion and autophagy after intracerebral injection of PGN. *A*) PGN or PBS was stereotaxically injected into the mouse CPU. At indicated time points after injections, coronal brain slices of 2.0 mm containing the CPU of one hemisphere were dissected. Tissue was homogenized, and CPU cells were costained with anti-CD45 (FITC), anti-CD11b (APC), AnV-PE (AnV), and 7-AAD and analyzed by flow cytometry gating on $CD11b^+$ $CD45^+$ microglial and macrophage cells. Bar graphs represents means ± SD of frequency of dead cells of 3 separate experiments. *B*) At indicated time points after injections, 10-μm brain sections were stained with an anti-CD45 (green) primary antibody and then with an Alexa Fluor 488 secondary antibody. Slides were analyzed under a laser scanning confocal fluorescence microscope. Arrowheads indicate parenchymal microglial and macrophage cells ($CD45^+$ stained cells). Bar graphs represent means ± SD of numbers of $CD45^+$ cells obtained from 10 fields/slide, analyzing the next 3 sections without the needle artifact of 3 separate experiments. $*P < 0.05$, $***P < 0.001$ *vs.* PBS-injected mice.

unrestricted tissue damage and degenerative disease may ensue. Until recently, 3 morphologically distinct types of cell death were recognized, including apoptosis (type I), autophagy (type II), and necrosis (type III). Necrosis was formerly considered to be an accidental, unregulated form of cell death resulting from excessive stress, although this may be an oversimplistic view, as necrosis may, under certain circumstances, involve the mobilization of specific signal transduction mechanisms. As a counterpart of uncontrolled necrosis, the term "programmed necrosis" (further named necroptosis) defines the forms of programmed cell death with necrotic morphology (48). The first described pathway leading to necroptosis is initiated by ligation of TNFR1 (48) in which, depending on the cell status, TNF-α administration results in caspase-dependent or caspase-independent programmed cell death (49). Therefore, we examined whether TNF-α was involved in PGN-induced microglial death. Although stimulation of microglial cells with TLR2 agonists increased the production of TNF-α, it also increased cell death in microglial cells in the presence of a monoclonal antibody specific for TNF-α and in microglial cells from TNFR1 KO mice. These results rule out the participation of TNF-α in the induction of microglial cell death.

It has been reported that activation of rat cortical astrocytes with LPS increases caspase-dependent apoptotic cell death *via* a nitric oxide-mediated mechanism (50). In contrast, hemin-induced cell death, although similarly dependent on increased NO production, occurs *via* caspase-independent necroptosis (51). Our studies showed that activation of TLR2 in microglial cells enhanced the expression of iNOS, which resulted in elevated nictric oxide production. However, inhibition of nitric oxide production with AG failed to reduce TLR2-induced microglial cell death.

Our TEM studies revealed that PGN was able induce disruption of outer cell membrane and numerous large cytoplasmic inclusions that were membrane-bound vacuoles characteristic of autophagy. Thus, it is plausible

that TLR2 stimulation in microglial cells may trigger autophagic cell death. Consistent with this, when microglial cells were activated with PGN and synthetic TLR2 ligands, the levels of LC3B II were increased, caspase-3 activation remained low, and two autophagy inhibitors, 3-MA and LY294002, were able to block microglial cell death. These results indicate that when microglial cells are activated with minor caspase activation, cell death may result from the autophagic pathway. Our findings are also consistent with previous findings that the pan-caspase inhibitor zVAD induces beclin-1-dependent autophagic cell death (11).

Stimulation of TLR4 with LPS activates to microglial cells with increased p53 expression, culminating in cell stress and apoptosis (52). However, activation of TLR4 in primary microglial cells with sublethal doses of LPS also sustained cell viability, without any measurable increase in apoptotic or necrotic cell death, therefore overcoming the induction of apoptosis *in vitro* (53). More recently, a novel aspect of TLR4 in microglial cells emerged demonstrating that activation of caspase-8 and caspase-3/7 was needed for activating the cells without cell death (22). This is in agreement with the findings that caspase-8 may suppress autophagic cell death (11). Thus, engagement of TLR4 may result in different outcomes depending on the amount of ligand available in the cell microenvironment and the activation of different set of regulatory caspases. Our studies demonstrated that engagement of another TLR family member, TLR2, fails to activate caspases but induces autophagic cell death. Therefore, the diversity of cell fate after TLRs stimulation becomes more complex if we consider different members of TLR family.

Microglial activation in the midbrain participates in neuroinflammatory and neurodegenerative responses in patients of Parkinson's disease (54) and in animal models of neurodegeneration induced by striatal injection of LPS (54). We demonstrated that intracerebral injection of TLR2 ligands increased both autophagy and death of microglial/macrophage cells and as a consequence the cell numbers were reduced into the brain parenchyma. These data are consistent with findings in *S. aureus*-induced brain abscess in which TLR2 on microglia reduced microglial cell population in the brain parenchyma (55). Moreover, granulocyte and macrophage recruitment was regulated by TLR2, as shown by hyperinflammation in TLR2-deficient animals (55). Thus, TLR2 may be exploited by the bacteria to evade innate host immune responses that may limit their colonization.

Our data revealed that stimulation of TLR2 in microglial cells initially activates the cells followed by the induction of autophagic cell death. Therefore, TLR2 has the potential to control microglial cell population, and this capacity might be exploited by pathogens to evade innate host immune responses. This novel role of TLR2 may also be utilized for the design of therapeutics to reduce the number of microglial cells that may exacerbate the pathogenic processes of neurodegenerative diseases. FJ

The authors thank biochemist Paula Icely for technical support and secretarial assistance. This work was supported by the Fogarty International Center, U.S. National Institutes of Health (HIH; grant 1R01TW007621); Consejo Nacional de Investigaciones Cientificas y Tecnicas, Argentina; and Secretaría de Ciencia y Tecnología, Universidad Nacional de Córdoba (SECyT-UNC), Argentina. Its contents are solely the responsibility of the authors and do not necessarily represent the official views of the Fogarty International Center, NIH. The authors declare no conflicts of interest.

REFERENCES

1. Mizushima, N., Levine, B., Cuervo, A. M., and Klionsky, D. J. (2008) Autophagy fights disease through cellular self-digestion. *Nature* **451,** 1069–1075
2. Mehrpour, M., Esclatine, A., Beau, I., and Codogno, P. (2010) Overview of macroautophagy regulation in mammalian cells. *Cell Res.* **20,** 748–762
3. Bursch, W., Karwan, A., Mayer, M., Dornetshuber, J., Frohwein, U., Schulte-Hermann, R., Fazi, B., Di Sano, F., Piredda, L., Piacentini, M., Petrovski, G., Fesus, L., and Gerner, C. (2008) Cell death and autophagy: cytokines, drugs, and nutritional factors. *Toxicology* **254,** 147–157
4. Maiuri, M. C., Zalckvar, E., Kimchi, A., and Kroemer, G. (2007) Self-eating and self-killing: crosstalk between autophagy and apoptosis. *Nat. Rev. Mol. Cell Biol.* **8,** 741–752
5. Nakagawa, I., Amano, A., Mizushima, N., Yamamoto, A., Yamaguchi, H., Kamimoto, T., Nara, A., Funao, J., Nakata, M., Tsuda, K., Hamada, S., and Yoshimori, T. (2004) Autophagy defends cells against invading group A Streptococcus. *Science* **306,** 1037–1040
6. Singh, S. B., Davis, A. S., Taylor, G. A., and Deretic, V. (2006) Human IRGM induces autophagy to eliminate intracellular mycobacteria. *Science* **313,** 1438–1441
7. Sanjuan, M. A., Dillon, C. P., Tait, S. W., Moshiach, S., Dorsey, F., Connell, S., Komatsu, M., Tanaka, K., Cleveland, J. L., Withoff, S., and Green, D. R. (2007) Toll-like receptor signalling in macrophages links the autophagy pathway to phagocytosis. *Nature* **450,** 1253–1257
8. Degterev, A., and Yuan, J. (2008) Expansion and evolution of cell death programmes. *Nat. Rev. Mol. Cell Biol.* **9,** 378–390
9. Lu, B., Capan, E., and Li, C. (2007) Autophagy induction and autophagic cell death in effector T cells. *Autophagy* **3,** 158–159
10. Yuan, J., Lipinski, M., and Degterev, A. (2003) Diversity in the mechanisms of neuronal cell death. *Neuron* **40,** 401–413
11. Yu, L., Alva, A., Su, H., Dutt, P., Freundt, E., Welsh, S., Baehrecke, E. H., and Lenardo, M. J. (2004) Regulation of an ATG7-beclin 1 program of autophagic cell death by caspase-8. *Science* **304,** 1500–1502
12. Nimmerjahn, A., Kirchhoff, F., and Helmchen, F. (2005) Resting microglial cells are highly dynamic surveillants of brain parenchyma in vivo. *Science* **308,** 1314–1318
13. Ponomarev, E. D., Maresz, K., Tan, Y., and Dittel, B. N. (2007) CNS-derived interleukin-4 is essential for the regulation of autoimmune inflammation and induces a state of alternative activation in microglial cells. *J. Neurosci.* **27,** 10714–10721
14. Wirenfeldt, M., Babcock, A. A., Ladeby, R., Lambertsen, K. L., Dagnaes-Hansen, F., Leslie, R. G., Owens, T., and Finsen, B. (2005) Reactive microgliosis engages distinct responses by microglial subpopulations after minor central nervous system injury. *J. Neurosci. Res.* **82,** 507–514
15. Hailer, N. P., Grampp, A., and Nitsch, R. (1999) Proliferation of microglia and astrocytes in the dentate gyrus following entorhinal cortex lesion: a quantitative bromodeoxyuridine-labelling study. *Eur. J. Neurosci.* **11,** 3359–3364
16. Rappert, A., Bechmann, I., Pivneva, T., Mahlo, J., Biber, K., Nolte, C., Kovac, A. D., Gerard, C., Boddeke, H. W., Nitsch, R., and Kettenmann, H. (2004) CXCR3-dependent microglial recruitment is essential for dendrite loss after brain lesion. *J. Neurosci.* **24,** 8500–8509
17. Soria, J. A., Arroyo, D. S., Gaviglio, E. A., Rodriguez-Galan, M. C., Wang, J. M., and Iribarren, P. (2011) Interleukin 4

induces the apoptosis of mouse microglial cells by a caspase-dependent mechanism. *Neurobiol. Dis.* **43,** 616–624
18. Vidlak, D., Mariani, M. M., Aldrich, A., Liu, S., and Kielian, T. (2011) Roles of Toll-like receptor 2 (TLR2) and superantigens on adaptive immune responses during CNS staphylococcal infection. *Brain Behav. Immun.* **25,** 905–914
19. Arroyo, D. S., Soria, J. A., Gaviglio, E. A., Rodriguez-Galan, M. C., and Iribarren, P. (2011) Toll-like receptors are key players in neurodegeneration. *Int. Immunopharmacol.* **11,** 1415–1421
20. O'Neill, L. A. (2006) How Toll-like receptors signal: what we know and what we don't know. *Curr. Opin. Immunol.* **18,** 3–9
21. Kielian, T., Esen, N., and Bearden, E. D. (2005) Toll-like receptor 2 (TLR2) is pivotal for recognition of S. aureus peptidoglycan but not intact bacteria by microglia. *Glia* **49,** 567–576
22. Burguillos, M. A., Deierborg, T., Kavanagh, E., Persson, A., Hajji, N., Garcia-Quintanilla, A., Cano, J., Brundin, P., Englund, E., Venero, J. L., and Joseph, B. (2011) Caspase signalling controls microglia activation and neurotoxicity. *Nature* **472,** 319–324
23. Iribarren, P., Correa, S. G., Sodero, N., and Riera, C. M. (2002) Activation of macrophages by silicones: phenotype and production of oxidant metabolites. *BMC Immunol.* **3,** 6
24. Rabinovich, G. A., Riera, C. M., and Iribarren, P. (1999) Granulocyte-macrophage colony-stimulating factor protects dendritic cells from liposome-encapsulated dichloromethylene diphosphonate-induced apoptosis through a Bcl-2-mediated pathway. *Eur. J. Immunol.* **29,** 563–570
25. Munafo, D. B., and Colombo, M. I. (2001) A novel assay to study autophagy: regulation of autophagosome vacuole size by amino acid deprivation. *J. Cell Sci.* **114,** 3619–3629
26. Franklin, K., and Paxinos, G. (2008) *The Mouse Brain in Stereotaxic Coordinates*, Academic Press, New York
27. Chen, K., Iribarren, P., Hu, J., Chen, J., Gong, W., Cho, E. H., Lockett, S., Dunlop, N. M., and Wang, J. M. (2006) Activation of Toll-like receptor 2 on microglia promotes cell uptake of Alzheimer disease-associated amyloid beta peptide. *J. Biol. Chem.* **281,** 3651–3659
28. Jung, D. Y., Lee, H., Jung, B. Y., Ock, J., Lee, M. S., Lee, W. H., and Suk, K. (2005) TLR4, but not TLR2, signals autoregulatory apoptosis of cultured microglia: a critical role of IFN-beta as a decision maker. *J. Immunol.* **174,** 6467–6476
29. Mayo, L., Jacob-Hirsch, J., Amariglio, N., Rechavi, G., Moutin, M. J., Lund, F. E., and Stein, R. (2008) Dual role of CD38 in microglial activation and activation-induced cell death. *J. Immunol.* **181,** 92–103
30. Olson, J. K., and Miller, S. D. (2004) Microglia initiate central nervous system innate and adaptive immune responses through multiple TLRs. *J. Immunol.* **173,** 3916–3924
31. Mayo, L., and Stein, R. (2007) Characterization of LPS and interferon-gamma triggered activation-induced cell death in N9 and primary microglial cells: induction of the mitochondrial gateway by nitric oxide. *Cell Death Differ.* **14,** 183–186
32. Fernandes-Alnemri, T., Litwack, G., and Alnemri, E. S. (1994) CPP32, a novel human apoptotic protein with homology to Caenorhabditis elegans cell death protein Ced-3 and mammalian interleukin-1 beta-converting enzyme. *J. Biol. Chem.* **269,** 30761–30764
33. Mann, S. S., and Hammarback, J. A. (1994) Molecular characterization of light chain 3. A microtubule binding subunit of MAP1A and MAP1B. *J. Biol. Chem.* **269,** 11492–11497
34. Mizushima, N., and Yoshimori, T. (2007) How to interpret LC3 immunoblotting. *Autophagy* **3,** 542–545
35. Kabeya, Y., Mizushima, N., Ueno, T., Yamamoto, A., Kirisako, T., Noda, T., Kominami, E., Ohsumi, Y., and Yoshimori, T. (2000) LC3, a mammalian homologue of yeast Apg8p, is localized in autophagosome membranes after processing. *EMBO J.* **19,** 5720–5728
36. D'Amours, D., Desnoyers, S., D'Silva, I., and Poirier, G. G. (1999) Poly(ADP-ribosyl)ation reactions in the regulation of nuclear functions. *Biochem. J.* **342,** 249–268
37. Gobeil, S., Boucher, C. C., Nadeau, D., and Poirier, G. G. (2001) Characterization of the necrotic cleavage of poly(ADP-ribose) polymerase (PARP-1): implication of lysosomal proteases. *Cell Death Differ.* **8,** 588–594
38. Girardin, S. E., Boneca, I. G., Viala, J., Chamaillard, M., Labigne, A., Thomas, G., Philpott, D. J., and Sansonetti, P. J. (2003) Nod2 is a general sensor of peptidoglycan through muramyl dipeptide (MDP) detection. *J. Biol. Chem.* **278,** 8869–8872
39. Mizutani, M., Pino, P. A., Saederup, N., Charo, I. F., Ransohoff, R. M., and Cardona, A. E. (2012) The fractalkine receptor but not CCR2 is present on microglia from embryonic development throughout adulthood. *J. Immunol.* **188,** 29–36
40. Aloisi, F. (2001) Immune function of microglia. *Glia* **36,** 165–179
41. Iribarren, P., Cui, Y. H., Le, Y., and Wang, J. M. (2002) The role of dendritic cells in neurodegenerative diseases. *Arch. Immunol. Ther. Exp. (Warsz.)* **50,** 187–196
42. Bezzi, P., Domercq, M., Brambilla, L., Galli, R., Schols, D., De Clercq, E., Vescovi, A., Bagetta, G., Kollias, G., Meldolesi, J., and Volterra, A. (2001) CXCR4-activated astrocyte glutamate release via TNFalpha: amplification by microglia triggers neurotoxicity. *Nat. Neurosci.* **4,** 702–710
43. Kreutzberg, G. W. (1996) Microglia: a sensor for pathological events in the CNS. *Trends Neurosci.* **19,** 312–318
44. Streit, W. J., Walter, S. A., and Pennell, N. A. (1999) Reactive microgliosis. *Prog. Neurobiol.* **57,** 563–581
45. Boddeke, E. W., Meigel, I., Frentzel, S., Gourmala, N. G., Harrison, J. K., Buttini, M., Spleiss, O., and Gebicke-Harter, P. (1999) Cultured rat microglia express functional beta-chemokine receptors. *J. Neuroimmunol.* **98,** 176–184
46. Jones, L. L., Banati, R. B., Graeber, M. B., Bonfanti, L., Raivich, G., and Kreutzberg, G. W. (1997) Population control of microglia: does apoptosis play a role? *J. Neurocytol.* **26,** 755–770
47. Wirenfeldt, M., Dissing-Olesen, L., Anne Babcock, A., Nielsen, M., Meldgaard, M., Zimmer, J., Azcoitia, I., Leslie, R. G., Dagnaes-Hansen, F., and Finsen, B. (2007) Population control of resident and immigrant microglia by mitosis and apoptosis. *Am. J. Pathol.* **171,** 617–631
48. Hitomi, J., Christofferson, D. E., Ng, A., Yao, J., Degterev, A., Xavier, R. J., and Yuan, J. (2008) Identification of a molecular signaling network that regulates a cellular necrotic cell death pathway. *Cell* **135,** 1311–1323
49. Delavallee, L., Cabon, L., Galan-Malo, P., Lorenzo, H. K., and Susin, S. A. (2011) AIF-mediated caspase-independent necroptosis: a new chance for targeted therapeutics. *IUBMB Life* **63,** 221–232
50. Suk, K., Lee, J., Hur, J., Kim, Y. S., Lee, M., Cha, S., Yeou Kim, S., and Kim, H. (2001) Activation-induced cell death of rat astrocytes. *Brain Res.* **900,** 342–347
51. Laird, M. D., Wakade, C., Alleyne, C. H., Jr., and Dhandapani, K. M. (2008) Hemin-induced necroptosis involves glutathione depletion in mouse astrocytes. *Free Radic. Biol. Med.* **45,** 1103–1114
52. Davenport, C. M., Sevastou, I. G., Hooper, C., and Pocock, J. M. (2010) Inhibiting p53 pathways in microglia attenuates microglial-evoked neurotoxicity following exposure to Alzheimer peptides. *J. Neurochem.* **112,** 552–563
53. Kaneko, Y. S., Nakashima, A., Mori, K., Nagatsu, T., Nagatsu, I., and Ota, A. (2009) Lipopolysaccharide extends the lifespan of mouse primary-cultured microglia. *Brain Res.* **1279,** 9–20
54. Choi, D. Y., Liu, M., Hunter, R. L., Cass, W. A., Pandya, J. D., Sullivan, P. G., Shin, E. J., Kim, H. C., Gash, D. M., and Bing, G. (2009) Striatal neuroinflammation promotes Parkinsonism in rats. *PLoS One* **4,** e5482
55. Stenzel, W., Soltek, S., Sanchez-Ruiz, M., Akira, S., Miletic, H., Schluter, D., and Deckert, M. (2008) Both TLR2 and TLR4 are required for the effective immune response in *Staphylococcus aureus*-induced experimental murine brain abscess. *Am. J. Pathol.* **172,** 132–145

Received for publication July 11, 2012.
Accepted for publication October 1, 2012.